Academic Journal of Science and Technology
ISSN: 2771-3032 | Vol. 22, No. 1, 2026

A Coupled Inductor Coil Z-Source Inverter for Photovoltaic-Assisted Charging of Hilly Electric Agricultural Machinery

Yunzhong Dai[1, 3], Shuangqiang Zhu[3, *], Wang Yi[3], Yuhan Xie[3], Shiyi Liu[1], Kangle Guo[1], Teng Ma[3]

[1]Intelligent Manufacturing Institute, Yibin Vocational and Technical College, Yibin 644100, China
[2]Department of Industrial Mining and Architecture, Bijie Vocational and Technical College, Bijie 551700, China
[3]School of Mechanical Engineering, Xihua University, Chengdu 610039, China

[*] Corresponding author: 2101708709@qq.com

Abstract: The coupled inductor coil Z-source inverter has advantages such as continuous input current and good boost performance. However, the traditional quasi-Z-source inverter not only requires a bulky isolation transformer but also suffers from large high-frequency common-mode leakage current. To address these drawbacks, this paper first proposes a coupled inductor coil Z-source inverter topology for photovoltaic-assisted charging of hilly electric agricultural machinery. Secondly, the high-frequency common-mode leakage current suppression mechanism of the inverter is analysed. Then, a detailed comparison is made between the proposed inverter and the traditional quasi-Z-source inverter. The research shows that the proposed inverter not only effectively suppresses high-frequency common-mode leakage current without the need for a bulky isolation transformer, but also requires only one magnetic core and one capacitor, which can effectively reduce the weight and volume of the inverter and lower its cost. Finally, the correctness of the inverter design and theoretical analysis is verified by circuit simulation.

Keywords: Coupled inductor coil Z-source inverter; hilly electric agricultural machinery; photovoltaic charging; leakage current.

1. Introduction

As a key connection link between the DC power supply side (lithium battery, photovoltaic) and the load side (AI processor, AC drive motor) in photovoltaic-assisted charging of hilly electric agricultural machinery, the performance of the inverter has a significant impact on the stability and safety of the entire machine [1-2]. Compared with traditional agricultural machinery, solar-assisted charging electric agricultural machinery significantly reduces the weight and volume of the whole machine and has better terrain adaptability, making it particularly suitable for mountainous and hilly operating environments [3-4]. To meet the requirements of intelligent control and power drive, the inverter must stably provide pure sinusoidal AC power to the AI processor and the AC drive motor, ensuring control accuracy and motor output quality [5-6].Traditional bridge inverters require dead time to be set for the switches on the same bridge arm to avoid arm short-circuit, but the introduction of dead time increases the harmonics of the grid-connected current and reduces power quality [7-8]. The quasi-Z-source bridge grid-connected inverter adds a unique impedance network between the input power supply and the inverter bridge, breaking the operation mode of the traditional bridge inverter, thereby allowing a shoot-through state in which the upper and lower bridge arms are simultaneously conductive [9]. Compared with DC-DC boost converters and dual-buck inverters, by reasonably inserting shoot-through vectors into the quasi-Z-source inverter bridge, the DC bus voltage can be effectively increased and the DC voltage utilisation rate can be improved. Compared with traditional two-stage inverter topologies, the quasi-Z-source bridge inverter can improve system efficiency, enhance reliability, and reduce cost [10]. However, new energy mountain intelligent agricultural machinery operates for long periods in outdoor, humid environments, facing unique electrical safety hazards. The parasitic capacitance of photovoltaic panels to ground can easily excite common-mode voltage in humid weather conditions, forming a leakage current path. This leakage current may trigger the protection mechanism, leading to equipment shutdown, or even threaten the electrical safety of the whole machine and cause injury to operators. The common-mode voltage of the traditional quasi-Z-source bridge inverter changes at high frequency, resulting in large common-mode leakage current. According to the German VDE-0126-1-1 standard, when the leakage current of the inverter exceeds 300 mA, the inverter must be disconnected from the AC side within 0.3 seconds [11-12]. Therefore, leakage current suppression is one of the key issues that must be addressed for inverters. In practical engineering, to suppress high-frequency common-mode leakage current, the traditional quasi-Z-source bridge inverter requires the installation of a bulky isolation transformer, which directly increases the system volume and cost, and reduces power density [13-14]. In addition, the bridge inverter must pass current through the body diode of the switch, which has poor performance, during the freewheeling stage, resulting in poor reliability and large reverse recovery losses [15].

To address the drawbacks of the existing quasi-Z-source bridge inverter, such as large high-frequency common-mode leakage current, the need for an isolation transformer that increases volume and cost, and large freewheeling losses, this paper first proposes a coupled inductor coil Z-source inverter topology for photovoltaic-assisted charging of hilly electric agricultural machinery. Then, its operation modes and common-mode leakage current suppression mechanism are analysed. Finally, the correctness of the inverter design is verified by circuit experiments.

2. Coupled Inductor Coil Z-Source Inverter for Photovoltaic-Assisted Charging of Hilly Electric Agricultural Machinery

2.1. Circuit Topology of the Novel Coupled Inductor Coil Z-Source Inverter

The circuit connection diagram of the coupled inductor coil Z-source inverter for photovoltaic charging of hilly electric agricultural machinery is shown in Figure 1. The inverter includes an RD snubber circuit, coupled inductor coils L, switches S_1–S_5, filter capacitor C_1, high-performance diode D_1, high-performance diode D_2, photovoltaic DC power supply U_{dc}, and a grid-side symmetrical filter circuit [5].

The two coupled inductor coils L are wound on the same magnetic core and connected in parallel on opposite sides. The dotted terminal of one coupled inductor coil L is connected to the positive terminal of the photovoltaic DC power supply U_{dc}, and the undotted terminal of the other coupled inductor coil L is connected to the negative terminal of U_{dc}. The filter capacitor C_1 is connected in series on the same side between the two coupled inductor coils L. The R_d snubber circuit includes a resistor R_d and a diode D_3. The grid-side symmetrical filter circuit includes an AC side voltage u_g, filter inductors L_3 and L_4, and switches S_3 and S_4.

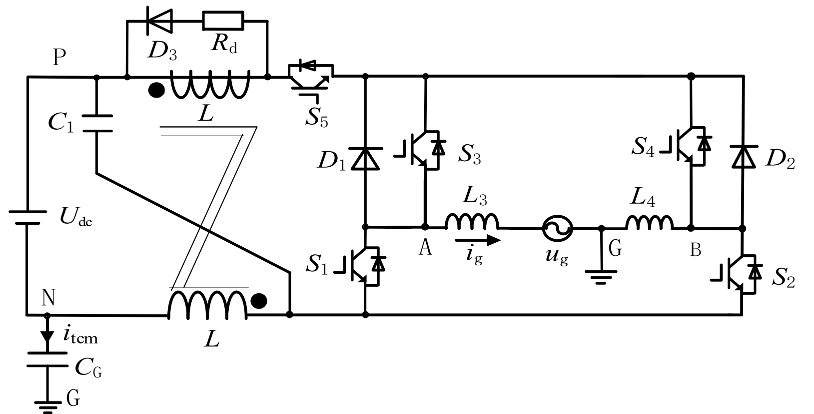

Figure 1. Circuit connection diagram of the coupled inductor coil Z-source inverter

2.2. Modulation Method of the Coupled Inductor Coil Z-Source Inverter

According to the topology of the coupled inductor coil Z-source inverter for photovoltaic-assisted charging of hilly electric agricultural machinery, a modulation strategy based on the polarity of the AC side current i_g and the drive signals of S_1–S_5 are designed, as shown in Figure 2. Here, i_g is the AC side current and u_g is the grid frequency. When $i_g > 0$, switches S_2, S_3 and S_5 are turned on, S_1 and S_4 remain off, $S_2 = S_3$, and $S_5 = S_2$. When $i_g < 0$, switches S_1, S_4 and S_5 are turned on, S_2 and S_3 remain off, $S_1 = S_4$, and $S_5 = S_1$ [6][7].

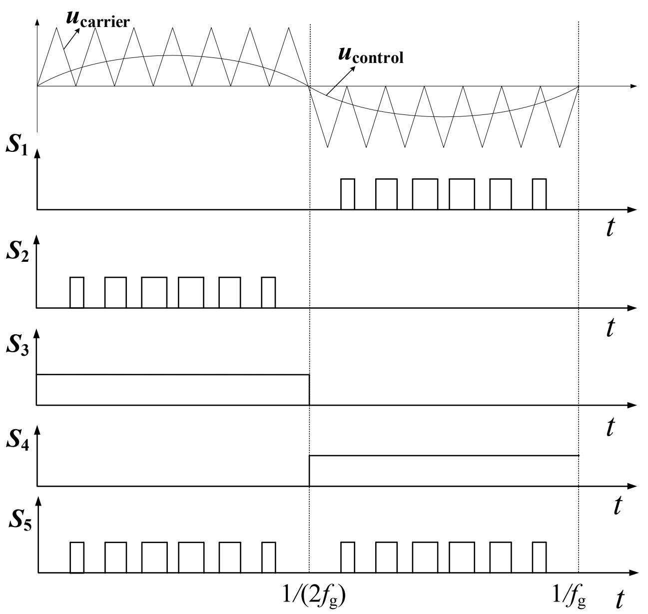

Figure 2. Drive waveforms of S_1–S_5 of the coupled inductor coil Z-source inverter

Therefore, from the above analysis, it can be seen that the coupled inductor coil Z-source inverter using one magnetic core and one capacitor can effectively reduce the weight and volume of the inverter and lower its cost.

3. Operation Modes and Common-Mode Leakage Current Analysis

3.1. Common-Mode Equivalent Circuit

Let i_g be positive when flowing from bridge arm midpoint A to point G. Since there is a parasitic capacitance from the photovoltaic panel to ground, its equivalent capacitance is C_G. C_G has the characteristic of blocking DC and passing AC, so the common-mode leakage current itcm is only related to the AC side voltage u_g. To eliminate differential-mode leakage current, let $L_3 = L_4 = L_1$. V_{NG} is the voltage across the distributed capacitor C_G, that is, the effective common-mode voltage. When the influence of the DC power supply U_{dc} on itcm is neglected, the common-mode equivalent circuit model of the coupled inductor coil Z-source inverter for photovoltaic charging of hilly electric agricultural machinery is shown in Figure 3 [8]. From Figure 1 and equation (1), it can be seen that itcm in the circuit is caused by the high-frequency variation of V_{NG}.

$$V_{NG} = \frac{(u_g - U_{dc})}{2} \quad (1)$$

where V_{NG} is the common-mode voltage.

3.2. Operation Modes and High-Frequency Common-Mode Leakage Current Analysis

To analyse the high-frequency common-mode leakage current of the coupled inductor coil Z-source inverter for photovoltaic charging of hilly electric agricultural machinery in the positive half-cycle and negative half-cycle respectively, let i_g be positive when flowing from point A to point G. According to the switching states of S_1–S_5 in Figures 1 and 2, the inverter can be divided into four operation modes, and their equivalent circuits are shown in Figures 3(a)–3(d), respectively [9][10].

Mode 1: Switches S_2, S_3 and S_5 are turned on, switches S_1 and S_4 are turned off, and the AC side current i_g provided by the AC side voltage usg is greater than 0. Its equivalent circuit is shown in Figure 3(a). From Figure 3(a), it can be seen that D_1 and D_2 are reverse-biased and turned off; U_{dc}, L, S_5, S_3, L_3, u_g, L_4 and S_2 form a forward charging closed loop, and i_g increases positively; D_3 is reverse-biased and turned off. Further, according to Figure 3(a) and Kirchhoff's voltage law, we obtain:

$$V_{NG} = u_g - U_{dc} - I_g \times j \times \omega_{SW} \times (\frac{L}{2} - L_3) \quad (2)$$

$$V_{NG} = I_g \times j \times \omega_{SW} \times (\frac{L}{2} - L_4) \quad (3)$$

In equations (2) and (3), V_{NG} is the voltage across the distributed capacitor C_G, that is, the effective common-mode voltage; $\omega_{SW} = 2\pi fg$, and I_g is the effective value of i_g. When $L_3 = L_4 = L_1$, according to equations (2) and (3), the common-mode voltage V_{NG} of the coupled inductor coil Z-source inverter for photovoltaic charging of hilly electric agricultural machinery in Mode I is:

$$V_{NG} = \frac{(u_g - U_{dc})}{2} \quad (4)$$

Mode 2: Switch S_3 and high-performance diode D_2 are turned on, high-performance diode D_1, switches S_1, S_2, S_4 and S_5 are turned off, and the AC side current I_g provided by the AC side voltage u_g is greater than 0. Its equivalent circuit is shown in Figure 3(b). R_d, D_3 and L form a forward Z-source network freewheeling loop, which quickly dissipates the energy of the Z-source network; L_3, u_g, L_4, D_2 and S_3 form a forward discharge freewheeling loop, and I_g decreases positively. This freewheeling path does not pass through the body diode of the switch, which has poor performance, reducing reverse recovery losses and improving inverter efficiency and reliability. From Figure 3(b), when S_5, S_3 and S_2 are the same type of switches, the voltage stresses of S_5, S_3 and S_2 are the same, that is:

$$V_{S_5} = V_{S_2} = V_{S_1} \quad (5)$$

In equation (5), V_{S5}, V_{S3} and V_{S2} are the voltages across switches S_5, S_3 and S_2, respectively. According to Figure 3(b) and Kirchhoff's voltage law, we obtain:

$$\begin{aligned} V_{S_2} + V_{S_5} &= U_{dc} \\ V_{S_1} + V_{S_5} &= U_{dc} \end{aligned} \quad (6)$$

Combining equations (5) and (6), we obtain:

$$V_{S_1} = V_{S_2} = V_{S_5} = \frac{U_{dc}}{2} \quad (7)$$

Furthermore, according to Figure 3(b) and Kirchhoff's voltage law, we obtain:

$$V_{NG} = u_g - V_{S_1} - I_g \times j \times \omega_{SW} \times (\frac{L}{2} - L_3) \quad (8)$$

$$V_{NG} = I_g \times j \times \omega_{SW} \times (\frac{L}{2} - L_4) - V_{S_2} \quad (9)$$

Similarly, when $L_3 = L_4 = L_1$, according to equations (7), (8) and (9), the common-mode voltage V_{NG} of the coupled inductor coil Z-source inverter for photovoltaic charging of hilly electric agricultural machinery in Mode 2 is:

$$V_{NG} = \frac{u_g - U_{dc}}{2} \quad (10)$$

Mode 3: Switches S_1, S_4 and S_5 are turned on, high-performance diodes D_1 and D_2, and switches S_2 and S_3 are turned off, and the AC side current i_g provided by the AC side voltage u_g is less than 0. Its equivalent circuit is shown in Figure 3(c). From Figure 3(c), it can be seen that U_{dc}, S_5, S_4, L_4, u_g, L_3, S_1 and L form a reverse charging closed loop, and i_g increases negatively; D_3 is reverse-biased and turned off. Furthermore, from Figure 3(c), the common-mode voltage V_{NG} of the coupled inductor coil Z-source inverter for photovoltaic charging of hilly electric agricultural machinery in Mode 3 is:

$$V_{NG} = -U_{dc} - I_g \times j \times \omega_{SW} \times (\frac{L}{2} - L_4) \quad (11)$$

$$V_{NG} = u_g + I_g \times j \times \omega_{SW} \times (\frac{L}{2} - L_3) \quad (12)$$

Similarly, when $L_3 = L_4 = L_1$, according to equations (11) and (12), the common-mode voltage V_{NG} of the coupled inductor coil Z-source inverter for photovoltaic charging of hilly electric agricultural machinery in Mode III is:

$$V_{NG} = \frac{u_g - U_{dc}}{2} \quad (13)$$

Mode 4: Switch S_4 and high-performance diode D_1 are turned on, switches S_1, S_2, S_3 and S_5 are turned off, and the AC side current i_g provided by the AC side voltage u_g is less than 0. Its equivalent circuit is shown in Figure 3(d). From Figure 3(d), it can be seen that S_4, D_4, u_g, L_g, L_1 and D_1 form a reverse discharge freewheeling loop; R_d, D_3 and L form a negative Z-source network freewheeling loop, which quickly dissipates the energy of the Z-source network; i_g decreases negatively. Further, according to Kirchhoff's voltage law, we obtain:

$$V_{NG} = -\frac{U_{dc}}{2} + u_g - I_g \times j \times \omega_{SW} \times (\frac{L}{2} - L_3) \quad (14)$$

$$V_{NG} = -\frac{U_{dc}}{2} + I_g \times j \times \omega_{SW} \times (\frac{L}{2} - L_4) \quad (15)$$

Similarly, when $L_3 = L_4 = L_1$, according to equations (14) and (15), the common-mode voltage V_{NG} of the coupled inductor coil Z-source inverter for photovoltaic charging of hilly electric agricultural machinery in Mode IV is:

$$V_{NG} = \frac{u_g - U_{dc}}{2} \quad (16)$$

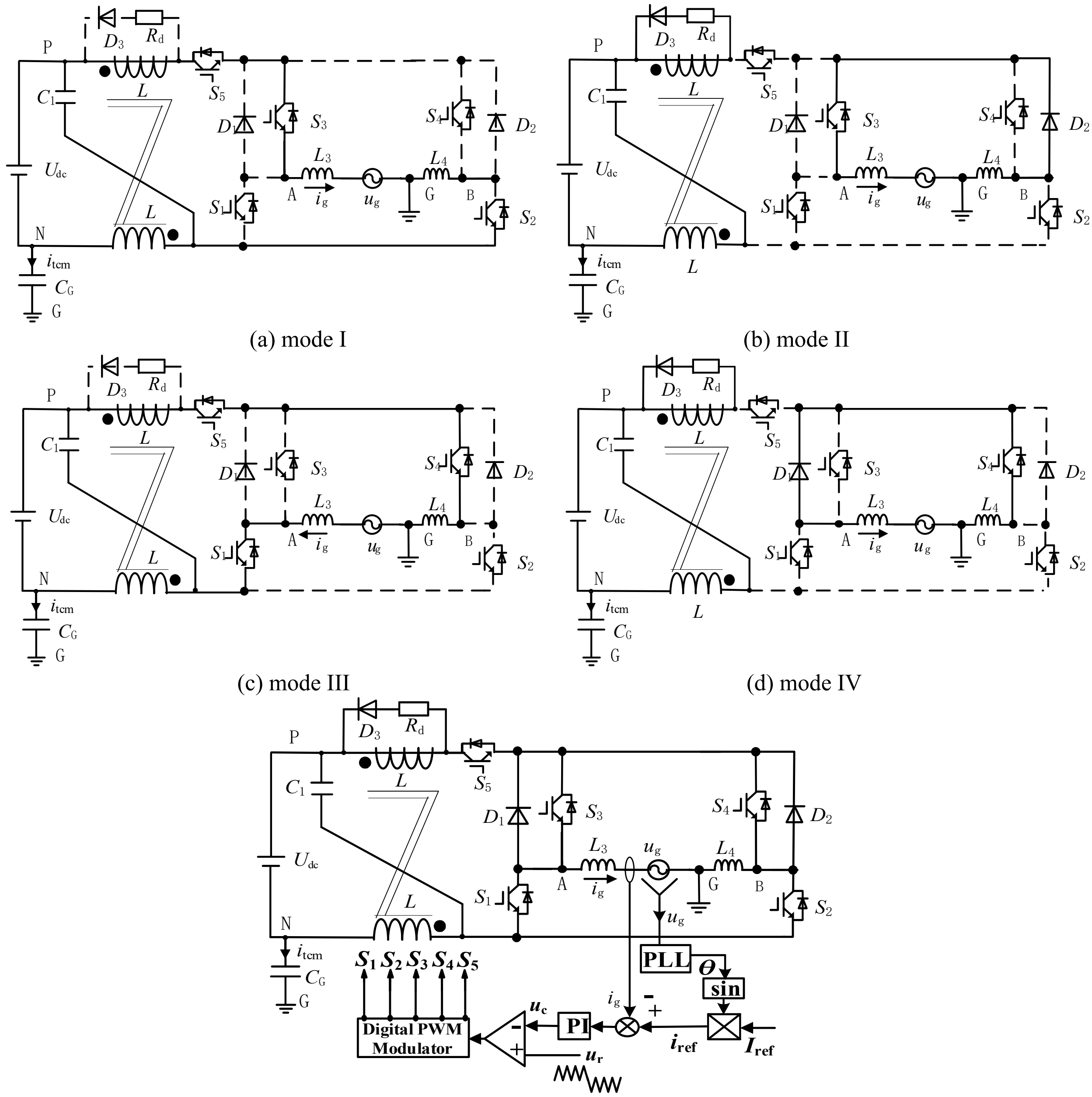

Figure 3. Operation modes and their equivalent circuits

From the above analysis, the operation modes and common-mode voltage V_{NG} of the coupled inductor coil Z-source inverter for photovoltaic charging of hilly electric agricultural machinery are shown in Table 1.

Table 1. Operation modes and common-mode voltage V_{NG}

	Half-cycle	Common-mode voltage (V_{NG})
Positive half-cycle	I	$V_{NG} = \frac{u_g - U_{dc}}{2}$
	II	$V_{NG} = \frac{u_g - U_{dc}}{2}$
Negative half-cycle	Half-cycle	Common-mode voltage (V_{NG})
	III	$V_{NG} = \frac{u_g - U_{dc}}{2}$
	IV	$V_{NG} = \frac{u_g - U_{dc}}{2}$

From Table 1, it can be seen that Modes 1 to 4 have the same common-mode voltage V_{NG} = (u_g - U_{dc})/2, which contains only DC and low-frequency components and has no high-frequency components. Therefore, the coupled inductor coil Z-source inverter for photovoltaic charging of hilly electric agricultural machinery and its unipolar modulation strategy proposed in this paper can effectively suppress the high-frequency common-mode leakage current of the inverter system while achieving high-quality sinusoidal AC output, without the need for a bulky isolation transformer, thereby reducing the weight, volume and cost of the inverter [11].

4. Simulation Verification

To verify the correctness of the topology and common-mode leakage current analysis of the coupled inductor coil Z-source inverter for photovoltaic charging of hilly electric agricultural machinery proposed in this paper, the inverter system of the present invention is adopted, using direct current control, as shown in Figure 4 [12].

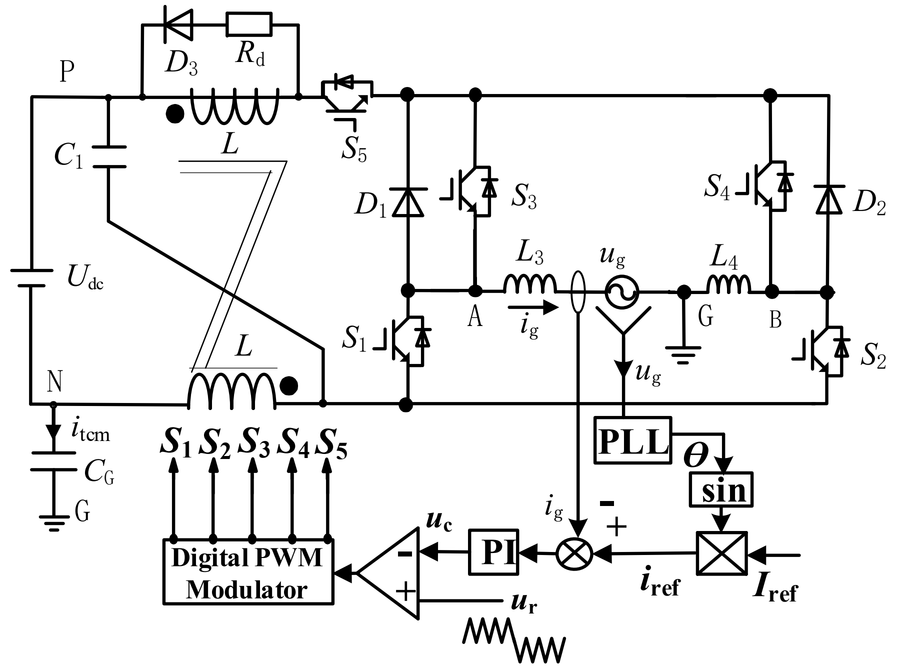

Figure 4. System circuit diagram of the coupled inductor coil Z-source inverter for photovoltaic charging of hilly electric agricultural machinery

The phase-locked loop circuit obtains the phase angle θ of u_g, and by executing the DSP program to look up the corresponding sine table data $sin\theta$, the reference signal of i_g is $i_{ref} = I_{ref} \times sin\theta$. The deviation value after comparing i_g and i_{ref} is passed through a PI regulator to obtain the modulation signal u_c, thereby achieving the same phase of u_g and i_g. The circuit simulation parameters of the coupled inductor coil Z-source inverter for photovoltaic charging of hilly electric agricultural machinery are shown in Table 2 [13].

Table 2. Circuit simulation parameters

Parameter	Value	Parameter	Value
U_{dc}	400V	C_G	75nF
U_m	220V	L_3=L_4	1.2mH
L	200uH	f_g	50Hz
f_s	5kHz	I_{ref}	15A
C_1	4000uF	R_d	2Ω

Using the above circuit simulation parameters, the waveforms of u_g and i_g can be obtained, as shown in Figure 5. u_g and i_g remain in the same phase, indicating that the coupled inductor coil Z-source inverter for photovoltaic charging of hilly electric agricultural machinery proposed in this paper has a high power factor.

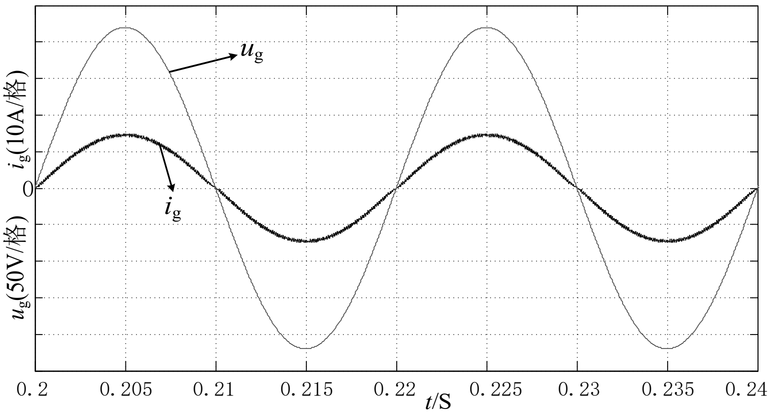

Figure 5. Simulation waveforms of i_g and u_g

Regarding the FFT analysis waveform of i_g, as shown in Figure 6, i_g is a sinusoidal waveform with relatively small waveform distortion, and the total harmonic distortion (THD) is 2.67%. Since there is no need to set dead time in the circuit simulation of the coupled inductor coil Z-source inverter for photovoltaic charging of hilly electric agricultural machinery, the figure shows that the harmonics are mainly concentrated near the switching frequency of 10 kHz, with few low-frequency harmonic components. Therefore, the coupled inductor coil Z-source inverter for photovoltaic charging of hilly electric agricultural machinery proposed in this paper has high grid-connected power quality.

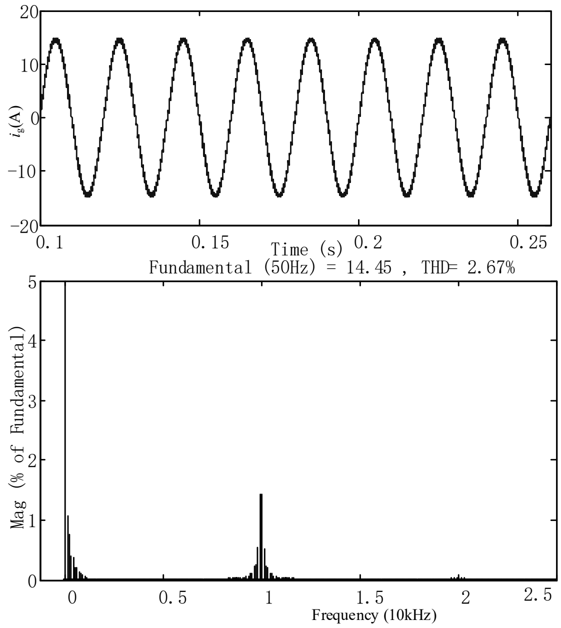

Figure 6. FFT analysis of i_g

Regarding the waveform of the effective common-mode voltage V_{NG}, as shown in Figure 7, the common-mode voltage V_{NG} contains only power frequency and DC components, with no high-frequency components, verifying the correctness of the common-mode voltage analysis of the coupled inductor coil Z-source inverter for photovoltaic charging of hilly electric agricultural machinery.

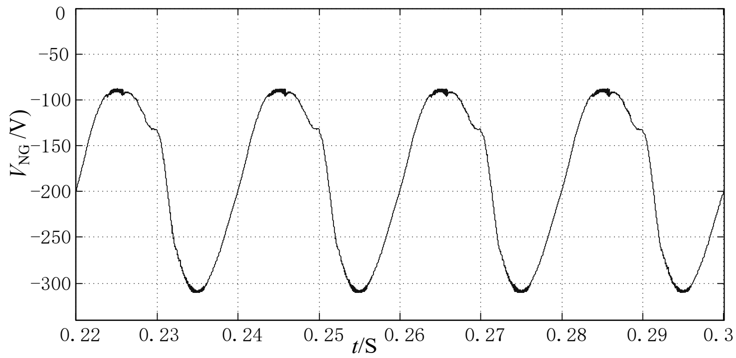

Figure 7. Simulation waveform of V_{NG}

Regarding the common-mode leakage current i_{tcm} waveform, as shown in Figure 8, the coupled inductor coil Z-source inverter for photovoltaic charging of hilly electric agricultural machinery provided in this paper has a peak value of approximately 52 mA within one power frequency cycle, which meets the requirements of the VDE-0126-1-1 standard for the leakage current of grid-connected inverters. Thus, the correctness of the topology design and common-mode leakage current analysis of the coupled inductor coil Z-source inverter for photovoltaic charging of hilly electric agricultural machinery is verified.

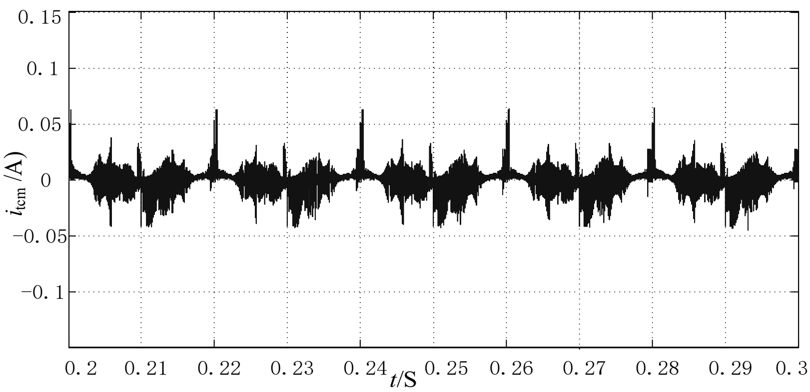

Figure 8. Simulation waveform of i_{tcm}

From the above analysis, it can be seen that within the power frequency cycle, the common-mode voltage V_{NG} of the four operation modes of the coupled inductor coil Z-source inverter for photovoltaic charging of hilly electric agricultural machinery is the same, containing only DC and low-frequency components, with no high-frequency components [14].

5. Conclusion

Through the study of the coupled inductor coil Z-source inverter and its magnetic integration characteristics proposed in this paper, the following conclusions can be drawn:

1. The inverter winds two sets of coupled inductor coils on the same magnetic core. Compared with the traditional quasi-Z-source inverter, one magnetic core can be saved, and the correct winding direction enables the magnetic fields of the two sets of coils to enhance each other, thereby increasing the effective inductance of the inductor.

2. When the number of turns of the two sets of coils is the same as that of the original design, ignoring the influence of leakage inductance, the inductance of the magnetically coupled coils will double, significantly improving the inductance utilisation per unit magnetic core.

3. If the inductance after coupling is kept the same as that of the original design, the number of coil turns can be reduced by 30%, which is beneficial for reducing copper loss and decreasing volume.

4. When air-core coupled inductors are used, magnetic coupling can reduce the weight of the inductor by approximately 25%. When magnetic core inductors are used, one magnetic core can be further saved, achieving a more significant weight reduction effect.

Funding

This work was supported by the Yibin Municipal Science and Technology Bureau Project "Topology and Leakage Current Suppression Technology of Multi-Degree-of-Freedom Adjustable Z-Source Crystalline Silicon Photovoltaic Grid-Connected Inverter" (2024MZ003); Guizhou Provincial Science and Technology Cooperation Program – Central Government-Guided Local Project(2026)026; the Bijie Vocational and Technical College Research Project (XS22ZRYB-04); and the Sichuan Postdoctoral Research Project Special Funding Program (TB2023025).

References

[1] Carrasco, J. M., Franquelo, L. G., Bialasiewicz, J. T., et al. (2006). Power-electronic systems for the grid integration of renewable energy sources: a survey. IEEE Transactions on Industrial Electronics, 53(4), 1002–1016. https://doi.org/10.1109/TIE.2006.878356.

[2] Kjaer, S. B., Pedersen, J. K., & Blaabjerg, F. (2005). A review of single-phase grid-connected inverters for photovoltaic modules. IEEE Transactions on Industry Applications, 41(5), 1292–1306. https://doi.org/10.1109/TIA.2005.853371

[3] Peng, F. Z. (2003). Z-source inverter. IEEE Transactions on Industry Applications, 39(2), 504–510. https://doi.org/10.1109/TIA.2003.808920

[4] Li, Y., Anderson, J., Peng, F. Z., et al. (2009). Quasi-Z-source inverter for photovoltaic power generation systems. In 2009 Twenty-Fourth Annual IEEE Applied Power Electronics Conference and Exposition (pp. 918–924). IEEE. https://doi.org/10.1109/APEC.2009.4802772

[5] Anderson, J., & Peng, F. Z. (2008). Four quasi-Z-source inverters. In 2008 IEEE Power Electronics Specialists Conference (pp. 2743–2749). IEEE. https://doi.org/10.1109/PESC.2008.4592360

[6] Shen, M., & Peng, F. Z. (2008). Operation modes and characteristics of the Z-source inverter with small inductance or low power factor. IEEE Transactions on Industrial Electronics, 55(1), 89–96. https://doi.org/10.1109/TIE.2007.909063

[7] Peng, F. Z., Shen, M., & Qian, Z. (2005). Maximum boost control of the Z-source inverter. IEEE Transactions on Power Electronics, 20(4), 833–838. https://doi.org/10.1109/TPEL.2005.850927

[8] Xiao, H., & Xie, S. (2010). Leakage current analytical model and application in single-phase transformerless photovoltaic grid-connected inverter. IEEE Transactions on Electromagnetic Compatibility, 52(4), 902–913. https://doi.org/10.1109/TEMC.2010.2064169

[9] Gonzalez, R., Lopez, J., Sanchis, P., et al. (2007). Transformerless inverter for single-phase photovoltaic systems. IEEE Transactions on Power Electronics, 22(2), 693–697. https://doi.org/10.1109/TPEL.2007.892120

[10] Yang, B., Li, W., Gu, Y., et al. (2012). Improved transformerless inverter with common-mode leakage current elimination for a photovoltaic grid-connected power system. IEEE Transactions on Power Electronics, 27(2), 752–762. https://doi.org/10.1109/TPEL.2011.2160359

[11] Li, W., Gu, Y., Luo, H., et al. (2015). Topology review and derivation methodology of single-phase transformerless photovoltaic inverters for leakage current suppression. IEEE Transactions on Industrial Electronics, 62(7), 4537–4551. https://doi.org/10.1109/TIE.2015.2399278

[12] Villalva, M. G., Gazoli, J. R., & Filho, E. R. (2009). Comprehensive approach to modeling and simulation of photovoltaic arrays. IEEE Transactions on Power Electronics, 24(5), 1198–1208. https://doi.org/10.1109/TPEL.2009.2013862

[13] Ciobotaru, M., Teodorescu, R., & Blaabjerg, F. (2006). A new single-phase PLL structure based on second order generalized integrator. In 2006 37th IEEE Power Electronics Specialists Conference (pp. 1–6). IEEE. https://doi.org/10.1109/PESC.2006.1711988

[14] Kerekes, T., Teodorescu, R., Rodriguez, P., et al. (2011). A new high-efficiency single-phase transformerless PV inverter topology. IEEE Transactions on Industrial Electronics, 58(1), 184–191. https://doi.org/10.1109/TIE.2009.2024092

[15] Yang, S., Lei, Q., Peng, F. Z., et al. (2009). Current-fed quasi-Z-source inverter with coupled inductors. In 2009 IEEE Energy Conversion Congress and Exposition (pp. 3683–3689). IEEE. https://doi.org/10.1109/ECCE.2009.5316489